A Near-resonance Decoupling Approach (NRDA) for Scattering Solution of Near Resonant Structures †

C. C. Lu and W. C. Chew

Center for Computational Electromagnetics
Electromagnetics Laboratory
Department of Electrical and Computer Engineering
University of Illinois
Urbana, IL 61801

Abstract

The equivalence principle is applied in combination with the method of moments to calculate the electromagnetic scattering from conducting objects containing near-resonant open-ended cavities. The presence of the cavity increases the the iteration number in conjugate gradient iterations due to the near-resonant modes and the multiple wave bounces inside the cavity. The equivalence principle is used to separate the cavity region from the rest of the object, allowing an independent solution of the cavity problem by a direct inversion algorithm using a recursive scheme. The solution of the cavity is then represented by a generalized admittance matrix. Numerical results for two-dimensional composite targets show that the iteration number can be reduced significantly for objects containing long cavities. This algorithm can also be applied to three-dimensional problems which will be reported in the future.

† This work was supported by the Air Force Office of Scientific Research under Grant No. F49620-96-1-0025, the National Science Foundation under Grant No. NSF ECS93-02145, and the Office of Naval Research under Grant No. DAAH04-93-G-0430.

Date: November 21, 1996. File: case2d_ccem.tex

1. Introduction

In the solution of electromagnetic scattering from arbitrary objects, the integral equation method followed by an iterative solver for the pertinent matrix equation is an important method. It is known that the dominant CPU time for iterative methods is the product of two factors: the time for each iteration, and the number of iteration required for a convergent result. The first factor can be significantly reduced by applying the fast algorithms [1-14]. The second factor usually depends on the problem geometry structures. In electromagnetic scattering problems, internal resonances, near resonances as in cavity modes, and multiple bounces of the waves will lead to large iteration numbers. The combined field integral equation (CFIE) can eliminate the slow convergence caused by the internal resonances. However, it does not rectify those caused by multiple bounces in open-ended cavities. Recently we conducted extensive calculations using MLFMA [12] for a model aircraft that contains an engine inlet. Above the frequency when the inlet supports one or more propagation modes, the iteration number for an iterative solver increases significantly compared to the same aircraft with the inlet sealed even though the number of unknowns for the cavity region is only a fraction of that for the entire problem. In high frequency methods, the multiple wave bounces are usually accounted for by ray expansion method and ray tracing method [15]. Even then, the inordinately large number of bounces in a cavity renders the use of ray-tracing method difficult for simulating waves in a cavity. Several hybrid methods [16-18] have also been reported for this problem in which low frequency methods are combined with a high frequency method to solve for the scattering solution from the cavity alone. No interior-exterior coupling was considered for these methods.

In this paper, we propose an algorithm that applies the equivalence principle and the method of moments to study the multiple wave bounces in an open-ended cavity, and to reduce the iteration number for an iterative solution of the problems. The idea is to apply the equivalence principle to separate the cavity region from the exterior region and solve the cavity problem by the method of moments with a direct solver. The solution to the interior problem is represented by a generalized admittance matrix called Y-matrix. The Y-matrix relates the electric current and the magnetic current on the aperture. This relation is then combined with the exterior boundary integral equation to solve for the induced currents on the exterior surface. As the cavity response is specified by the Y-matrix where multiple-bounce wave physics has already been incorporated, the iteration process for the exterior problem is free from having to account for multiple-bounce physics inside the cavity. Consequently, the iteration count for the exterior solution is greatly reduced. We call this method the near-resonant decoupling approach (NRDA) because it decouples the near-resonance in the cavity region from the exterior surface using the equivalence principle. It is a rigorous method and the only approximation is the result of the numerical implementation.

Using the equivalence principle to study cavity scattering has also been studied by other authors [19-21]. In [19], the generalized admittance matrices for the interior and exterior regions are formulated. The formulation in [20] fails at internal resonant frequencies. The work in [21] studied the scattering problems for cavities embedded in an infinite ground plane. To our knowledge, no low-frequency method has been reported using the near-resonant decoupling approach (NRDA) to solve the combined interior and exterior problems. Hence our approach is focused on using the generalized admittance matrix to account for the cavity interaction with the exterior surface. The purpose of this study is to reduce the overall iteration number for the entire problem, and to reduce the total CPU time also in the case when the number of interior unknowns is a small fraction of that of the entire problem. In the following, we first introduce the formulation of this method for a general problem. Then we apply it to a two-dimensional problem.

2. General Formulation

The problem is to calculate electromagnetic scattering from a conducting object with an open-ended cavity due to an exterior incident field $\mathbf{E}^{inc}$. The boundary integral equation approach for this problem is to solve for the induced current distribution on the object surface (including the cavity wall and the exterior surface, see Figure 1) by solving the surface integral equation. For the problem in this paper, the object surface consists of two parts: (1) the interior surface (cavity wall), and (2) the exterior surface. The coupling between the interior and the exterior surface is through the aperture. Since the cavity interior structure gives rise to slow convergence of the entire problem due to multiple wave bounces, we decouple the cavity region from the rest of the object surface. To this end, we seal the aperture by a conducting sheet, and put electric and magnetic currents on both sides of the conducting sheet. Based on the equivalence principle, when the currents on the artificial conducting sheet are properly determined, the new configuration is exactly equivalent to the original one in that they give the same scattered field. As a result, the interior wall and the exterior surface are separated, and the original problem is converted into two problems: the interior problem, and the exterior problem. Two integral equations can be formulated for each problem.

The exterior equivalence problem is shown in Figure 1(b). In this case, the boundary integral equation is specified by

$$(\mathbf{E}^{sca} + \mathbf{E}^{inc}) \times \hat{n} = \mathbf{M}, \qquad \text{or} \qquad (\mathbf{E}^{sca} + \mathbf{E}^{inc})|_{\tan} = \hat{n} \times \mathbf{M}. \tag{1}$$

where $\mathbf{M}$ is the magnetic current distribution. It is zero outside the aperture region. The scattered field is related to $\mathbf{J}$ and $\mathbf{M}$ by

$$\mathbf{E}^{sca} = i\omega\mu \left[\int_S g\mathbf{J}\, dS' + \frac{\nabla}{k^2} \int_S g\nabla' \cdot \mathbf{J}\, dS' \right] - \nabla \times \int_S g\mathbf{M}\, dS'. \tag{2}$$

where $g = \exp(ik|\mathbf{r} - \mathbf{r}'|)/4\pi|\mathbf{r} - \mathbf{r}'|$ is the free space Green's function.

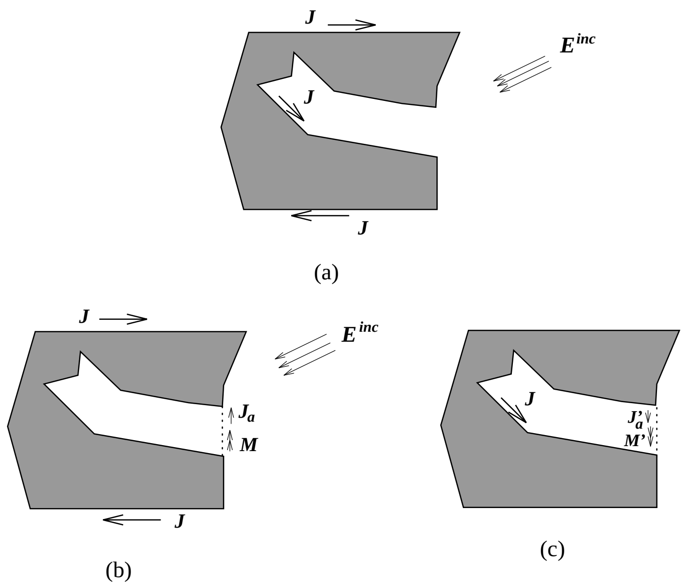

Figure 1. *(a) An open-ended cavity embedded in a conducting body. (b) External equivalence. (c) Interior equivalence.*

Equation (1) can be converted into matrix form using the method of moments,

$$\overline{\mathbf{G}}_{11} \cdot \mathbf{J} + \overline{\mathbf{G}}_{12} \cdot \mathbf{M} = \mathbf{V}. \tag{3}$$

where $\overline{\mathbf{G}}_{11}$ and $\overline{\mathbf{G}}_{12}$ are the matrix representation of the integral operators for $\mathbf{J}$ and $\mathbf{M}$, respectively, and $\mathbf{V}$ is the array calculated using the incident field $\mathbf{E}^{inc}$.

The integral equation for the interior equivalence problem can be formed in the similar manner, as shown in Figure 1(c). The electric and magnetic currents are $\mathbf{J}'$ and $\mathbf{M}'$ on the interior surface (now including the cavity wall and the aperture), respectively, with $\mathbf{M}' = 0$ on the cavity wall. A similar integral equation as (1) can be formed in terms of $\mathbf{J}'$ and $\mathbf{M}'$, and then converted into matrix form as

$$\overline{\mathbf{G}}'_{11} \cdot \mathbf{J}' + \overline{\mathbf{G}}'_{12} \cdot \mathbf{M}' = 0. \tag{4}$$

Equations (3) and (4) cannot be solved independently as the interior and the exterior regions are physically connected to each other. Also, there are more equations than unknowns in both equations. More equations can be introduced by using the continuity condition on the aperture:

$$\mathbf{J} = -\mathbf{J}', \qquad \mathbf{M} = -\mathbf{M}'. \tag{5}$$

Now that we have enough equations to determine all the unknowns, we first solve Equation (4) using, for example, Gauss elimination, to get

$$\mathbf{J}' = -\left(\overline{\mathbf{G}}'_{11}\right)^{-1} \cdot \overline{\mathbf{G}}'_{12} \cdot \mathbf{M}', \tag{6}$$

where $\mathbf{J}' = [\mathbf{J}'_a, \mathbf{J}'_w]$, and $\mathbf{J}'_a$ and $\mathbf{J}'_w$ stand for the current on the interior aperture and the interior wall, respectively. To couple the interior solution to the exterior problem, we need only the response $\mathbf{J}'_a$ on the aperture. Therefore, we calculate $\mathbf{J}'_a$ from (6) by

$$\mathbf{J}'_a = \overline{\mathbf{Y}} \cdot \mathbf{M}'. \tag{7}$$

Considering Equation (5), and let $\mathbf{J} = [\mathbf{J}_a, \mathbf{J}_w]$, we have

$$\mathbf{J}_a = \overline{\mathbf{Y}} \cdot \mathbf{M}. \tag{8}$$

Equation (8) can be interpreted as the cavity response to the impressed source $\mathbf{M}$ where multiple wave bounce physics has already been accounted for. For any aperture source distribution $\mathbf{M}$, the cavity response $\mathbf{J}_a$ can be calculated via the Y-matrix. Thus, the introduction of the Y-matrix allows the cavity to be treated as a black box within which the wave interactions are very complicated. However the influence of these interactions to the outside structure is via the precomputed aperture Y-matrix. For a relatively small cavity, a matrix inversion can be used to calculate the Y-matrix. When the cavity is very long and the matrix inversion cost is high, the inversion can be done recursively by dividing the cavity into several sections [21]. As a result, the cost of for solving the interior problem can be reduced.

Next we can solve the exterior integral equation. Combining (8) with (3) we get

$$\begin{bmatrix} \overline{\mathbf{G}}_{11} & \overline{\mathbf{G}}_{12} \\ \overline{\mathbf{G}}_{21} & -\overline{\mathbf{Y}} \end{bmatrix} \cdot \begin{bmatrix} \mathbf{J} \\ \mathbf{M} \end{bmatrix} = \begin{bmatrix} \mathbf{V} \\ 0 \end{bmatrix}, \tag{9}$$

where

$$\overline{\mathbf{G}}_{21} = \left[\underbrace{\overline{\mathbf{I}}}_{N_a \times N_a} \quad \underbrace{0}_{N_a \times (N - N_a)} \right], \tag{10}$$

and N_a is the number of unknowns on the aperture. Since the multiple-bounce wave physics inside the cavity has been accounted for by direct matrix inversion, and the interaction information is contained in the Y-matrix, the iterative solution to Equation (9) is now free from the influence of the interior multiple wave bounces. Hence, the required iteration number essentially depend on the exterior structures. In addition, the equivalent exterior problem has less unknowns than the original integral equation for the entire object.

The algorithm introduced above applies to general problems. In the next section, we present several simulation results for two dimensional problems.

3. Two-Dimensional Case

We have implemented the near-resonance decoupling algorithm (NRDA) for two dimensional problems. We use the method of moments with the pulse basis and point matching technique to discretize the integral equation. The code was implemented for an arbitrary two-dimensional objects. All the results presented are based on the combined field integral equation.

The first object is a rectangular cavity embedded in a rectangular cylinder, as shown in Figure 2. The object geometry is characterized by three parameters: aperture size 2a, cavity depth c, and thickness b. The frequency is 300 MHz for this simulation. This geometry has a closed form response for the electric current in terms of the impressed magnetic current. If an equivalent magnetic current

$$\mathbf{M}(y) = \hat{y} M_0 \sin k_y (y - a), \qquad k_y = \frac{m\pi}{2a}, \tag{11}$$

is applied on the aperture at $x = 0$, then we can show that the excited current distribution on the same aperture is given by

$$\mathbf{J}(y) = \hat{z} M_0 \frac{ik_x}{\eta k} \frac{\cos(k_x c)}{\sin(k_x c)} \sin k_y (y - a), \qquad k_x^2 = k^2 - k_y^2. \tag{12}$$

We now compare the current calculated from Equation (8) with that from (12). The comparison is made for the case with $a = 1.1\lambda$, $b = 0.2\lambda$, and $c = 0.31\lambda$. The plots for the current magnitudes are shown in Figure 3, demonstrating good agreement between the two results.

For this object, we then compared the RCS with that of the entire model solution, which is defined as the solution of the integral equation for the entire object surface with the same discretization and the iterative solver. The entire model solution is not the exact solution. However, the comparison reveals the error made through the numerical realization of the equivalence principle. The geometry parameters for this comparison are: $a = 1\lambda$, $b = 0.5\lambda$, and $c = 12\lambda$. The incident angle is 45^o from x-axis. Both TE and TM cases are shown in Figure 4. The agreement between the entire model solution and the solution of NRDA is excellent.

The goal of the NRDA is to reduce the iteration number required for the iterative solution of the matrix equation for a scatterer embedded with an open-ended cavity. We conducted this test for a rectangular cavity by fixing the parameters $a = 2.0\lambda$ and $b = 0.5\lambda$, respectively, and varying the depth parameter c. As seen from Figure 5, for the same problem and the same residual error in the conjugate gradient iteration, the iteration number required for NRDA is much smaller than that for the entire model solution. As is expected, as the cavity depth increases, the iteration number for the entire model solution also increases. On the contrary, the iteration number increase for NRDA is relatively small, and this increase is mainly due to the larger number of unknowns in the exterior problem.

As is mentioned in Section 2, when the cavity depth is much larger than the aperture, the interior solution (Y-matrix) can be obtained using the recursive scheme to reduce the solution time. We present three cases for the rectangular cavity to examine this concept. Each case uses different parameters: (1) $a = 4\lambda$, $b = 0.5\lambda$, $c = 15.30\lambda$, (2) $a = 2\lambda$, $b = 0.5\lambda$, $c = 15.10\lambda$, (3) $a = 0.75\lambda$, $b = 0.5\lambda$, $c = 20.30\lambda$. Since b is fixed, each case is characterized by a parameter $L/A = c/2a$ (this parameter is called the aspect ratio). For each case, we divide the cavity into different number of sections and record the total CPU time. The results are plotted in Figure 6. We observed that the reduction in the CPU time is significant for the first few divisions. However, excessive division will result in the increase in the CPU time. This can be explained as follows: In the recursive algorithm, each recursive step involves a matrix inversion. The size of the matrix is equal to the number of unknowns in that section (which includes the unknowns on the aperture as well as the wall). When the number of unknowns on the wall is not dominant (comparable or smaller than that for the aperture), much of the CPU time will be spent on the part of the matrix corresponding to the aperture unknowns.

Next we apply the algorithm to a more complicated structure as shown in Figure 7. The cavity cross section in this case contains straight lines as well as curved lines. The contour is specified by the coordinates (x_i, y_i), $i = 1, 2, ..., 13$ that are given in Table 1. The frequency used for this simulation is 600 MHz, the angle of incidence is 45^o. Because this is a test code, it cannot perform automatic partitioning of the cavity. We input the geometry data from an input file for two cases: Division 1 and Division 2. Division 1 stands for the case where the cavity is considered as one section. Division 2 means that the cavity is divided into two sections by connecting point 8 and point 12 as shown by the dash line in Figure 7. The RCS comparison between the model solution and NRDA are shown in Figure 8. Calculation shows that to achieve the residual error of 0.005, NRDA requires 19 iteration for both Division 1 and Division 2, while the entire model solution takes more than 200 iterations. The iteration histories are shown in Figure 9. Also plotted in this figure is the iteration history of the entire model solution for the same object with exterior surface only (solid rectangular cylinder). It is seen that the NRDA iteration history is almost the same as that for the exterior surface only. This once again demonstrates that the algorithm is essentially free from the influence of the interior cavity multiple wave bounces and near resonances.

One may argue that for the iterative solution for the entire model case, the matrix size is larger than that for NRDA, and hence the latter requires less iteration number and part of the computation for NRDA is shifted to solve the interior problem. This argument is true only for cases where the interior problem size is comparable or larger than the exterior problem and the aspect ratio L/A is small. In many practical structures such as the engine inlet of an aircraft, the interior problem size is usually a small fraction of the entire problem size, and the aspect ratio is large. In this case, the exterior problem consumes most part of the total CPU time. For the example of Figures 8 and 9, the number of interior and exterior unknowns are $N_i = 632$ and $N_o = 576$, respectively (note that N_i is slightly larger than N_o). The total CPU time for the model solution on a DEC Alpha workstation is 179.1 s. On the same machine, NRDA used the total CPU time 162.8 s. for one division, and 68.7 s. for two divisions (the iteration numbers for both cases of NRDA are 19).

4. Conclusion

Equivalence principle method has been combined with the method of moments to calculate the scattering from conducting objects with near-resonant open-ended cavity. This method has successfully been applied to solve for the scattering solution from two-dimensional cavities. The numerical calculations show that this method has significantly reduced the iteration number in the iterative solution for problems that are plagued by multiple wave bounces and near-resonance in an open-ended cavity. The algorithm divides the problem into interior and exterior problems, and hence the total solution time consists of two parts. For a target with large aspect ratio cavity, or for problems where exterior unknowns are dominant, this algorithm will also reduce the total CPU time.

References

[1] V. Rokhlin, "Rapid solution of integral equations of scattering theory in two dimensions," *J. Comput. Phys.*, vol. 86, no. 2, pp. 414-439, February 1990.

[2] R. Coifman, V. Rokhlin, and S. Wandzura, "The fast multipole method for the wave equation: a pedestrian prescription," *IEEE Antennas Propagat. Mag.*, vol. 35, no. 3, pp. 7-12, June 1993.

[3] A. Brandt, "Multilevel computations of integral transforms and particle interactions with oscillatory kernels," *Comput. Phys. Commun.*, vol. 65, pp. 24-38, 1991.

[4] N. Engheta, W. D. Murphy, V. Rokhlin, and M. S. Vassiliou, "The fast multipole method (FMM) for electromagnetic scattering problems," *IEEE Trans. Antennas Propagat.*, vol. 40, no. 6, pp. 634-641, July 1992.

[5] B. Dembart and E. Yip, "A 3D moment method code based on fast multipole," *URSI Radio Sci. Meet. Dig.*, p. 23, 1994.

[6] R. Coifman, V. Rokhlin, and S. Wandzura, "Faster single-stage multipole method for the wave equation," *10th Annual Review of Progress in Applied Computational Electromagnetics*, pp. 19-24, 1994.

[7] E. Michielssen and A. Boag, "Multilevel evaluation of electromagnetic fields for the rapid solution of scattering problems," *Microwave Opt. Tech. Lett.*, vol. 7, no. 17, pp. 790-795, December 1994.

[8] E. Michielssen and A. Boag, "A multilevel matrix decomposition algorithm for analyzing scattering from large structures," *11th Annual Re-*

view of Progress in Applied Computational Electromagnetics, pp. 614-620, 1995.

[9] H. Kim and H. Ling, "On the application of fast wavelet transform to the integral-equation solution of electromagnetic scattering problems," *Microwave Opt. Tech. Lett.*, vol. 6, no. 3, pp. 168-173, 1993.

[10] C. C. Lu and W. C. Chew, "Fast algorithm for solving hybrid integral equations," *IEE Proceedings-H*, vol. 140, no. 6, pp. 455-460, Dec. 1993.

[11] C. C. Lu and W. C. Chew, "A multilevel algorithm for solving boundary integral equations of wave scattering," *Microwave Opt. Tech. Lett.*, vol. 7, no. 10, pp. 466-470, July 1994.

[12] J. M. Song and W. C. Chew, "Multilevel fast-multipole algorithm for solving combined field integral equations of electromagnetic scattering," *Microwave Opt. Tech. Lett.*, vol. 10, no. 1, pp. 15-19, September 1995.

[13] F. X. Canning, "Transformations that produce a sparse moment method matrix," *J. Electromagn. Waves and Appl.*, vol. 4, no. 9, pp. 903-913, 1990.

[14] F. X. Canning, "Robust use of supplementary conditions for moment method solution near internal resonances," *IEEE Trans. Antennas Propagat.*, vol. 43, no. 3, March 1995.

[15] H. Ling, R. C. Chou, and S. W. Lee, "Shooting and bouncing rays: calculating the RCS of an arbitrary shaped cavity," *IEEE Trans. Antennas Propagat.*, vol. 37, no. 2, pp. 194-205, Feb. 1989.

[16] R. J. Burkholder and P. H. Pathak, "High-frequency electromagnetic scattering by open-ended waveguide cavities," *Radio Science*, vol. 26, no. 1, pp. 211-218, Jan.-Feb. 1991.

[17] D. C. Ross, J. L. Volakis, and H. T. Anastassiu, "Hybrid finite element-modal analysis of jet engine inlet scattering," *IEEE Trans. Antennas Propagat.*, vol. 43, no. 3, pp. 277-286, March 1995.

[18] J.-M. Jin and J. L. Volakis, "A finite element-boundary integral formulation for scattering by three-dimensional cavity-backed apertures," *IEEE Trans. Antennas Propagat.*, vol. 39, no. 1, pp. 97-104, Jan. 1991.

[19] R. F. Harrington and J. R. Mautz, "A generalized network formulation for paerture problems," *IEEE Trans. Antennas Propagat.*, vol. 24, no. 11, pp. 870-873, Nov. 1976.

[20] T. Wang, R. F. Harrington, and J. R. Mautz,"Electromagnetic scattering from and transmission through arbitrary apertures in conducting bodies," *IEEE Trans. Antennas Propagat.*, vol. 38, no. 11, pp. 1805-1814, Nov. 1990.

[21] T. -M. Wang and H. Ling, "Electromagnetic scattering from three-dimensional cavities via a connection scheme," *IEEE Trans. Antennas Propagat.*, vol. 39, no. 10, pp. 1505-1513, Oct. 1991.

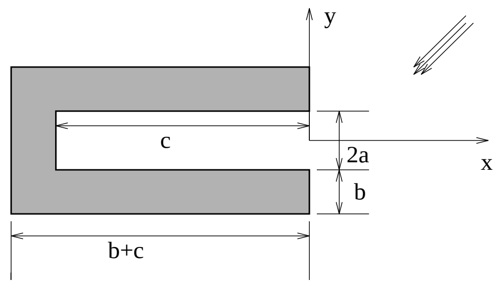

Figure 2. *A demonstration problem: The object is a 2D PEC cylinder with an open-ended cavity, defined by three parameters a, b, and c. The plane wave incident angle is* 45^o *with a frequency of* 300 *MHz. RCS for both TE and TM polarizations are presented.*

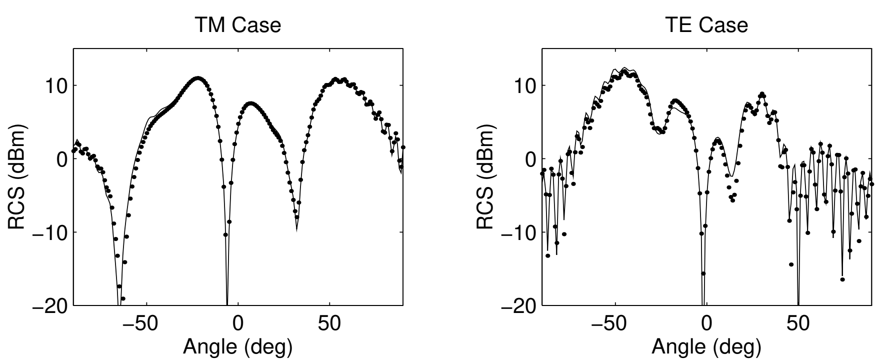

Figure 4. *The RCSs of the object in Figure 2 for* $a = 1\lambda$, $b = 0.5\lambda$, $c = 12.0\lambda$ *. The solid line is the RCS of the entire model solution, the dotted line is that of the algorithm in this paper (the cavity is divided into four sections of equal length). In this figure, the solid line is for the entire model solution, and the dotted line is for NRDA.*

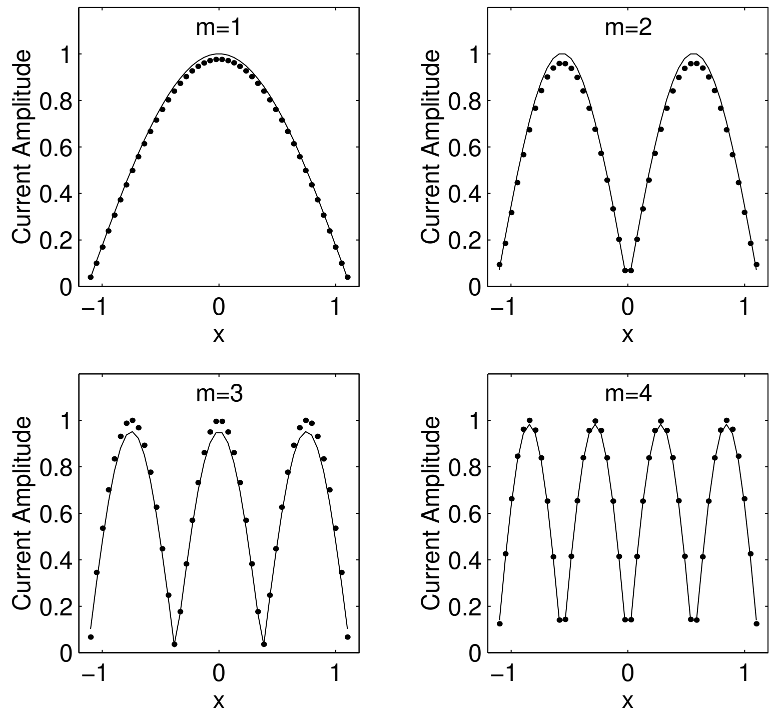

Figure 3. *The current distribution on the aperture. The dotted line is the result by Y-matrix. The solid line is the exact result calculated using Equation (12). The cavity size is* $0.31\lambda \times 2.2\lambda$ *(corresponding to* $a = 1.1\lambda$ *and* $c = 0.31\lambda$ *in Figure 2.)*

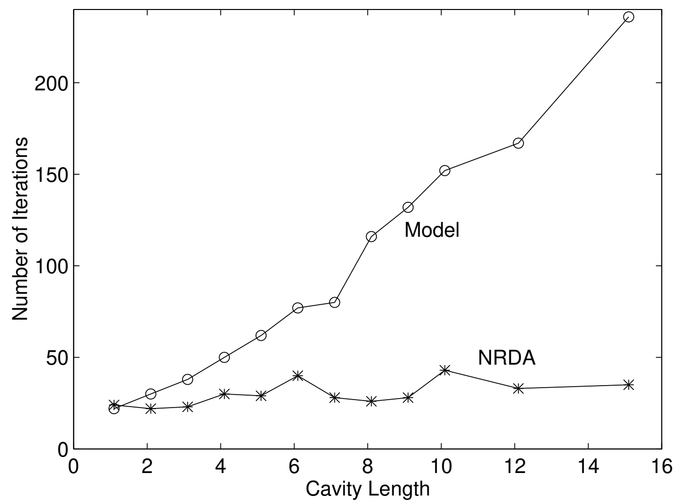

Figure 5. *The iteration number comparison for the model solution and NRDA for the object shown in Figure 2. The parameters* $a = 2\lambda$ *and* $b = 0.5\lambda$ *are fixed, and* c *is varying. The result is for TM polarization.*

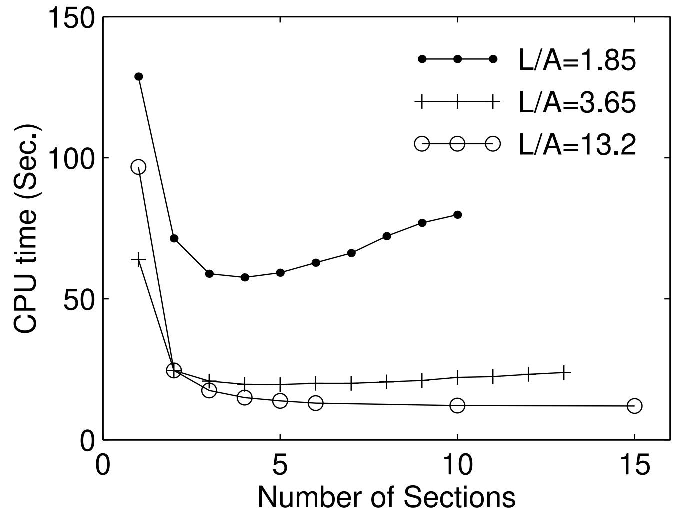

Figure 6. *The CPU time of the total solution vs the number of divisions of the cavity. The solid line is the RCS of the model solution, the dotted line is that of NRDA. The horizontal axis is the number of divisions, the vertical axis is the total CPU time (Sec.) on a DEC ALPHA work station. (The incident wave is in TM polarization).*

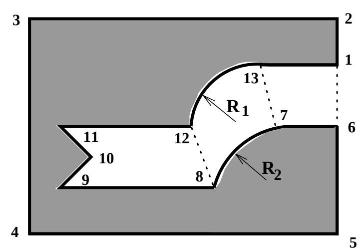

Figure 7. *The cross section of a two-dimensional object containing an open-ended cavity. The geometry is specified by a set of points with coordinates (x_i, y_i). For the simulation in this paper, the values (x_i, y_i) are listed in Table 1.*

i	1	2	3	4	5	6	7
x	0	0	-9	-9	0	0	-1.2
y	1.0	1.6	1.6	-4.8	-4.8	-1	-1

i	8	9	10	11	12	13
x	-4.4	-8.4	-8.4	-8.4	-6.0	-1.2
y	-4.2	-4.2	-3,.2	-2.2	-2.2	1

(R1=5.2,   R2=3.2)

Table 1. *The geometry data for the object in Figure 7.*

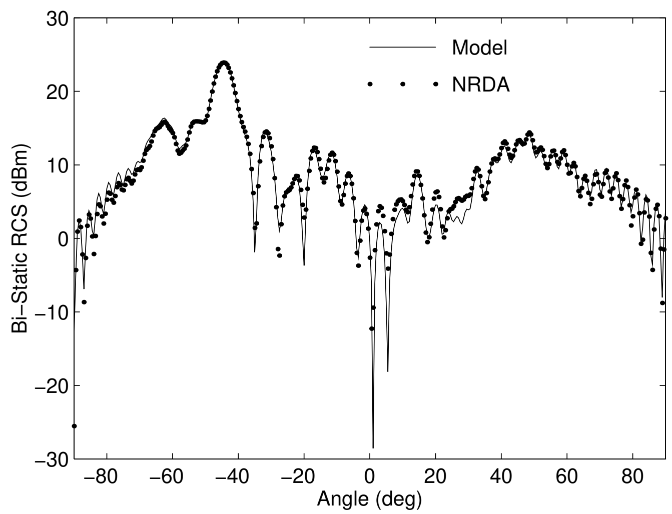

Figure 8. *The RCS of the object in Figure 7. The object geometry data are listed in Table 1. Other parameters are: frequency=600 MHz, incident angle = 45^o, incident wave polarization is TE.*

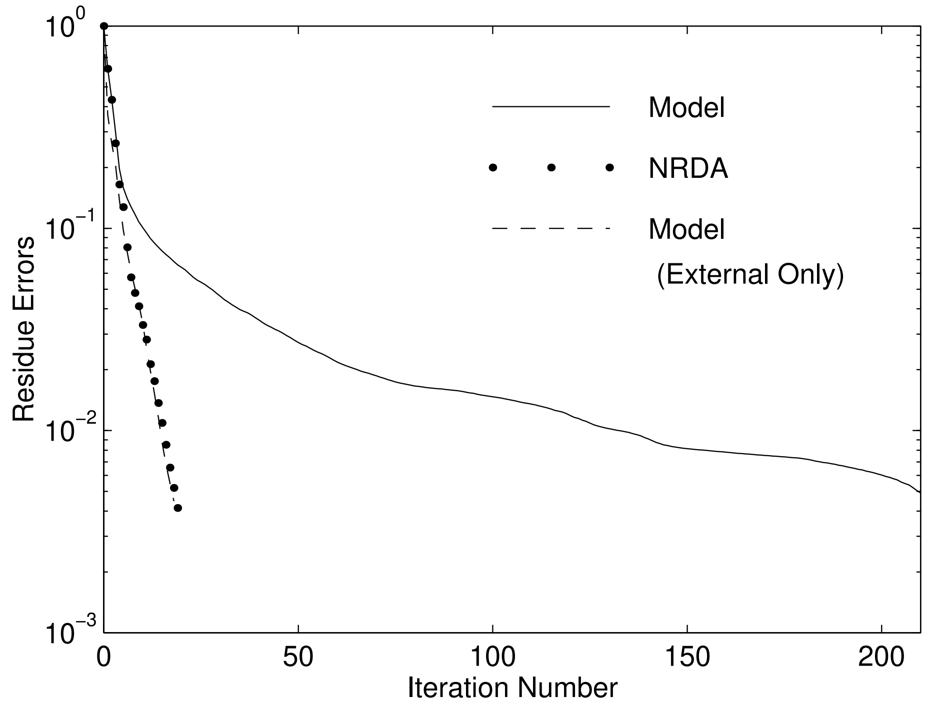

Figure 9. *The iteration histories for NRDA and the entire model solution for the object of Figure 7. Other parameters are the same as that of Figure 8. The iteration history is also plotted as dash line for the entire model solution for a solid rectangular with exactly the same surface as that of the exterior (closed) surface of the object in Figure 7.*